Physica Status Solidi B: Basic Solid State Physics

On the effect of magnetostatic interaction on the collective motion of vortex domain walls in a pair of nanostripes

--Manuscript Draft--

Manuscript Number:	pssb.201900113R2
Full Title:	On the effect of magnetostatic interaction on the collective motion of vortex domain walls in a pair of nanostripes
Article Type:	Original Paper
Section/Category:	
Keywords:	Nanostripe; magnetic vortex; domain wall; resonance
Corresponding Author:	Orlov Vitaly Krasnoyarsk, RUSSIAN FEDERATION
Additional Information:	
Question	**Response**
Please submit a plain text version of your cover letter here.	Dear edition. Please take into consideration our revised manuscript. V. Orlov, A. Ivanov I. Orlova
Do you or any of your co-authors have a conflict of interest to declare?	No. The authors declare no conflict of interest.
Corresponding Author Secondary Information:	
Corresponding Author's Institution:	
Corresponding Author's Secondary Institution:	
First Author:	Orlov Vitaly
First Author Secondary Information:	
Order of Authors:	Orlov Vitaly
	Ivanov Anatoly
	Orlova Irina
Order of Authors Secondary Information:	
Abstract:	The periodic motion of interacting vortex domain walls in a pair of nanostripes has been analytically and numerically investigated. A model consisting of two parallel nanostripes with the domain magnetization structure has been proposed, where domains are separated by vortex walls. The magnetic subsystems of the stripes magnetostatically interact, which causes the existence of normal magnetic vortex motion modes in the latter. Frequencies of the collective magnetization modes have been calculated using empirical expressions for the magnetic energy of interaction between vortex walls. It is shown that not any combinations of the polarity and chirality lead to the resonance magnetization behavior in ac fields.

physica status solidi

On the effect of magnetostatic interaction on the collective motion of vortex domain walls in a pair of nanostripes

Vitaly A. Orlov[*,1,2], Anatoly A. Ivanov[1], Irina N. Orlova[3]

[1] Siberian Federal University, Krasnoyarsk, 660041 Russia
[2] Kirensky Institute of Physics, Krasnoyarsk Scientific Center, Russian Academy of Sciences, Siberian Branch, Krasnoyarsk, 660036 Russia
[3] Krasnoyarsk State Pedagogical University after V.P. Astafev, Krasnoyarsk, 660049 Russia

Key words: Nanostripe, magnetic vortex, domain wall, resonance

[*] Corresponding author: e-mail orlhome@rambler.ru

The periodic motion of interacting vortex domain walls in a pair of nanostripes has been analytically and numerically investigated. A model consisting of two parallel nanostripes with the domain magnetization structure has been proposed, where domains are separated by vortex walls. The magnetic subsystems of the stripes magnetostatically interact, which causes the existence of normal magnetic vortex motion modes in the latter. Frequencies of the collective magnetization modes have been calculated using empirical expressions for the magnetic energy of interaction between vortex walls. It is shown that not any combinations of the polarity and chirality lead to the resonance magnetization behavior in ac fields.

1 Introduction Close attention of researchers to quasi-two-dimensional objects, including nanowires and nanostripes, is due to both the prospects of their use in designing various spintronic devices [1–3] and the possibility of solving many fundamental problems of magnetism of low-dimensional magnets. Special interest is focused upon magnetization switching of such objects. At the same time, the analytical description of the magnetic properties faces essential computational difficulties caused by a complex structure of stripe and wire magnetization. To solve particular problems and understand the processes occurring in nanostripes upon magnetization switching, computer simulation is often used.

The domain structure evolution in nanostripes in an applied ac magnetic field has attracted considerable interest. The structure of domain walls (DWs) in these magnets is extremely diverse and exhibits a complex behavior in dc and ac magnetic fields. Depending on the geometry of stripes (the ratio between their linear sizes) and their magnetic characteristics, DWs of different types are implemented, including conventional Neel (transverse) walls (TWs), vortex walls (VWs), and their complex combinations [4–9]. Different types of DWs have been intensively theoretically (see, for example, [10]) and experimentally (see, for example, [11]) investigated. Obviously, the motion of DWs with such complex configurations is accompanied by intriguing effects and attracts attention of researchers. In particular, several modes of VW motion under the action of a dc field or spin-polarized current of different values were found and fairly well-studied [12–16]. Interestingly, the vortex structure underlies the cyclic wall motion with displacements, i.e., the drift.

In arrays of adjacent wires (stripes), the mutual effect of magnetic subsystems of the latter cannot be excluded. The interaction between topological magnetization inhomogeneities is significant and affects magnetization switching [17, 18]. The aim of this work was to describe the cyclic VW motion in a pair of magnetostatically interacting nanostripes under the action of an ac magnetic field applied in the stripe plane. In addition, we discuss the effect

of a dc magnetic field applied perpendicular to the stripe plane. The formalism of the description of magnetic vortex behavior in ac fields as topological inhomogeneities has been fairly well-developed (see, for example, [19–30] and references therein). The analytical calculations are based on representing the Landau–Lifshitz equations in collective variables [31,32], specifically, the velocity and coordinates of the magnetic vortex core. The core is a region of the strongly inhomogeneous magnetization directed perpendicular to the magnet surface. In a magnetic field, it behaves as a quasiparticle and is formed by the competition between the exchange and magnetostatic energy.

The core magnetization state is usually specified by the two parameters: polarity $p = \pm 1$ and chirality $q = \pm 1$. The polarity sign is conventionally specified parallel or antiparallel to the stripe surface normal. The chirality sign is also conventional: clock- or counterclockwise magnetization rotation. To specify the vortex magnetic state, it is often convenient to use the parameter $\pi_T = pq$. In nanomagnets, the core moves as if a quasiparticle is affected by the gyroscopic force $\mathbf{F}_G = \mathbf{G} \times \mathbf{v}$. Here, $\mathbf{G}$ – is the gyrovector and $\mathbf{v}$ – is the core velocity.

The gyrovector value is determined as $|\mathbf{G}| = \pi_T(2\pi M_S b/\gamma)(1 - ph)$, where b is the magnet thickness, γ is the gyromagnetic ratio, M_S is the saturation magnetization, and $h = H/(\mu_0 M_S)$ is the dimensionless field applied perpendicular to the magnet plane (parallel or antiparallel to the magnetization at the core center) [24, 32]. The VWs in wires and stripes are also affected by this force.

To describe the VW motion, we should first derive the analytical expression for a core quasiparticle potential.

2 Effective Energy of a Vortex Domain Wall in the Stripe To solve the equation of magnetization motion, it is necessary to establish to have a functional dependence of the potential energy of a stripe magnetic subsystem on the generalized parameters. It is difficult to obtain a strict analytical form of the dependence of energy on the vortex core coordinate. In such systems, the energy of interacting VWs can be, at best, approximately presented as a system of interacting dipoles (quadrupoles). In such an approximation, the energy is expressed via complex integrals (see, for example, [10]), but near the equilibrium, the energy is quadratic with respect to the wall coordinates [13]. The results important for application are often obtained using computer simulation [6, 13, 14, 33–35].

Now, let us derive an empirical expression for the potential energy as a function of the core coordinate $W_M(\mathbf{r})$. We consider a model consisting of two parallel ferromagnetic stripes with thickness b and width L ($b \ll L$). The distance between the stripes is d. The lengths of the stripes exceed by far their width and thickness. The system of coordinates and model used are presented in Fig. 1. The magnetization distribution in nanostripes with the domain structure is formed by the competition between several energy types, including the exchange, demagnetizing, and anisotropy energies. In the general case, a DW can consist of regions with the traditional Neel-type magnetization rotation and a vortex region [36, 37]. Below, we present the qualitative considerations that specify a model magnetization distribution in a complex wall consisting of a TW and a VW.

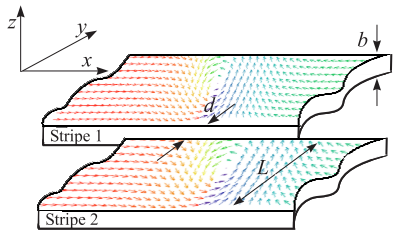

Figure 1 Model of a pair of parallel stripes.

We assume the magnetization distribution in the transition region between domains to result from superposition of TWs and VWs. This is, however, not a formal sum of the TW and VW vectors. Here, we should take into account that the absolute value of magnetization does not change with coordinate and the characteristic correlation radius of magnetization in a vortex is a finite quantity (the degree of the core effect on the magnetization direction decreases fairly fast with distance). In studies [38–41]), different descriptions of the spatial magnetization distribution in the vortex structures were reported. It is worth noting that the use of different types of anzats in the calculation does not affect the qualitative conclusions in describing the vortex structures. Therefore, to describe the correlation between the magnetizations in the core and at distance $\mathbf{r}$ from it, we use the dependence of the perpendicular magnetization component m_z on the coordinate from [41]:

$$m_z = \xi(\mathbf{r}, \delta_c) = \frac{1-h}{1+0.6\frac{\mathbf{r}^2}{\delta_c^2}} \exp\left(-0.1\frac{\mathbf{r}^2}{\delta_c^2}\right) + h. \quad (1)$$

The dimensionless dc field h is applied along the z axis, $|\mathbf{r}| = \sqrt{(x-X)^2 + (y-Y)^2}$, X and Y are the vortex core center coordinates, and $\delta_c \approx \sqrt{A/(\mu_0 M_S^2)}$ is the characteristic length of the perpendicular magnetization component decrease.

We present the components of the magnetization unit vector in the form

$$m_{x,y} = a_0 \left(m_{x_{vort},y_{vort}} + m_{x_{tr},y_{tr}}\right). \quad (2)$$

Here, $m_{x_{vort}}$ and $m_{y_{vort}}$ are the x and y components for the case of only the VW available, $m_{x_{tr}}$ and $m_{y_{tr}}$ are the magnetization components in the TW [37], and the normalization parameter a_0 is determined from the condition $m_z^2 + m_x^2 + m_y^2 = 1$. We assume the stripe thickness to be so small that the magnetization is independent of coordinate z. The expressions for the corresponding components

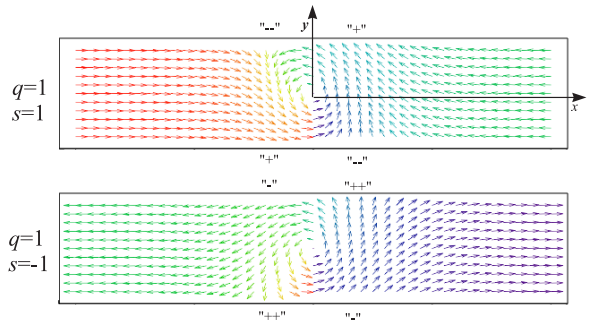

Figure 2 Example of the magnetization distribution in the vortex wall at different combinations of parameters q and s at $\delta_w = L$ and $\delta_c = 0.2\delta_w$.

are

$$m_{x_{vort}} = -\frac{y\xi(\mathbf{r},\delta_w)}{\sqrt{x^2+y^2}}, \qquad m_{y_{vort}} = \frac{x\xi(\mathbf{r},\delta_w)}{\sqrt{x^2+y^2}},$$
$$m_{x_{tr}} = s\tanh\left(\frac{x-X}{\delta_w}\right), \qquad m_{y_{tr}} = \sqrt{1-m_{x_{tr}}^2}. \tag{3}$$

Here, the parameter $s = \pm 1$ determines the magnetization direction in domains. The quantity δ_w determines the correlation magnetization length in the xy plane. It is reasonable to suggest that the difference between the quantities δ_c and δ_w is determined by the difference between the components of the tensor of demagnetizing factors along the z and y axes (N_z and N_y respectively). This allows us to assume $\delta_w/\delta_c \approx \sqrt{N_z/N_y}$ [42]. Thus, using Eq. (2), for the required magnetization component we obtain

$$m_y(x,y,X,Y) = \sqrt{1-\xi(\mathbf{r},\delta_c)^2}\times$$
$$\times\left(q(x-X)\xi(\mathbf{r},\delta_w) + m_{y_{tr}}|\mathbf{r}|\right) / \left[\mathbf{r}^2(1+\xi(\mathbf{r},\delta_w)^2) + \right.$$
$$\left. +2q\xi(\mathbf{r},\delta_w)|\mathbf{r}|\left((x-X)m_{y_{tr}} - (y-Y)m_{x_{tr}}\right)\right]^{1/2}. \tag{4}$$

The examples of magnetization distribution calculated using Eq. (4) are shown in Fig. 2, where the arrow lengths are proportional to the projection of the magnetization unit vector onto the xy plane. Note that the concept of the configuration of a magnetic field of the magnetostatic charge on the lateral stripe surface as a quadrupole (charge/dipole/quadrupole complex systems) is not quite correct. The region charge of localization on the stripe lateral surfaces is fairly large and comparable with stripe width L. It can be seen that the surface charge densities σ on the lateral surface are noticeably different in their absolute value in the regions with the positive and negative signs. In Fig. 2 , the regions with the higher density are shown by double symbols "++" "−−"and the regions with the lower density, by single symbols "+" "−". The same feature was observed for the field distribution in real wires [11].

Now, let us consider the mechanism of the occurrence of conservative forces acting on the core. At the vortex core displacement, the surface charge density distribution on the stripe lateral surface changes. This leads to the variation in the intrinsic energy of the stripes and their magnetostatic interaction W_M. Hence, the effective forces acting on the vortex cores of stripes 1 and 2, as in the case of quasiparticles, can be written in the form $\mathbf{F}_\alpha(\mathbf{r}_1,\mathbf{r}_2) = -\mathrm{grad}_\alpha(W_M(\mathbf{r}_1,\mathbf{r}_2))$ (subscript α is the stripe number and $\mathbf{r}_1$ and $\mathbf{r}_2$ are the radius vectors of the vortex centers in local systems of coordinates). In the estimations, it is convenient to use the rigid vortex model, in which the change in the magnetization distribution profile upon slight variation in the core coordinate is ignored [43–45]. For the energy of the magnetic subsystem of a pair of stripes, we obtain

$$W_M(X_1,X_2,Y_1,Y_2) = W_{1_{\text{self}}}(X_1,Y_1) + \\ +W_{2_{\text{self}}}(X_2,Y_2) + W_{\text{int}}(X_1,X_2,Y_1,Y_2). \tag{5}$$

In the right-hand side of Eq. (5), the first term $W_{1_{\text{self}}}(X_1,Y_1)$ describes the intrinsic energy of the first stripe without interaction with the magnetization of the second stripe. In Eq. (5) $W_{2_{\text{self}}}(X_2,Y_2)$ is the intrinsic energy of the second stripe and $W_{\text{int}}(X_1,X_2,Y_1,Y_2)$ is the term describing the interaction between the stripe magnetic subsystems. We write this expression in more detail. For each stripe, we use a local system of coordinates. For example, for the first stripe, we can write:

$$W_{1_{\text{self}}}(X_1,Y_1) = \frac{\mu_0 b^2}{4\pi}\int\limits_{-\infty}^{\infty}\int\limits_{-\infty}^{\infty}\frac{\sigma_1(x_1,X_1,Y_1)\sigma_2(x_2,X_1,Y_1)dx_1dx_2}{\sqrt{L^2+(x_1-x_2)^2}} + \\ +\frac{\mu_0 b^2}{4\pi}\int\limits_{-\infty}^{\infty}\int\limits_{-\infty}^{\infty}\frac{\sigma_1(x_1,X_1,Y_1)\sigma_1(x_2,X_1,Y_1)dx_1dx_2}{2|x_1-x_2|} + \\ +\frac{\mu_0 b^2}{4\pi}\int\limits_{-\infty}^{\infty}\int\limits_{-\infty}^{\infty}\frac{\sigma_2(x_1,X_1,Y_1)\sigma_2(x_2,X_1,Y_1)dx_1dx_2}{2|x_1-x_2|}, \tag{6}$$

or

$$W_{1_{\text{self}}}(U_1,V_1) = \\ = \frac{\mu_0 b^2 M_S^2}{4\pi L}\left[\int\limits_{-\infty}^{\infty}\int\limits_{-\infty}^{\infty}\frac{m_y\left(u_1,-\frac{1}{2},U_1,V_1\right)m_y\left(u_2,\frac{1}{2},U_1,V_1\right)du_1du_2}{\sqrt{1+(u_1-u_2)^2}} + \right. \\ + \int\limits_{-\infty}^{\infty}\int\limits_{-\infty}^{\infty}\frac{m_y\left(u_1,-\frac{1}{2},U_1,V_1\right)m_y\left(u_2,-\frac{1}{2},U_1,V_1\right)du_1du_2}{2|u_1-u_2|} + \\ \left. + \int\limits_{-\infty}^{\infty}\int\limits_{-\infty}^{\infty}\frac{m_y\left(u_1,\frac{1}{2},U_1,V_1\right)m_y\left(u_2,\frac{1}{2},U_1,V_1\right)du_1du_2}{2|u_1-u_2|}\right]. \tag{7}$$

Here, we passed to the dimensionless parameters $u_{1,2} = x_{1,2}/L$, $U_{1,2} = X_{1,2}/L$, and $V_{1,2} = Y_{1,2}/L$. In the framework of this model, the charge density on the stripe lateral surfaces (Fig. 2) can be written in the form $\sigma_1(x,X,Y) = M_S m_y\left(x,\frac{L}{2},X,Y\right)$, $\sigma_2(x,X,Y) = M_S m_y\left(x,-\frac{L}{2},X,Y\right)$. The first term in Eq. (7) describes the energy of interaction between charges from the opposite lateral surfaces and the second and third terms describe the interaction between the charges on one surface. Similarly, we can write the expression for the intrinsic energy of the second stripe.

The energy of interaction between the magnetizations in a pair of stripes is expressed as

$$W_{\text{int}}(U_1,V_1,U_2,V_2) = \\ = \frac{\mu_0 b^2 M_S^2}{4\pi L}\left[\int\limits_{-\infty}^{\infty}\int\limits_{-\infty}^{\infty}\frac{m_y\left(u_1,-\frac{1}{2},U_1,V_1\right)m'_y\left(u_2,-\frac{1}{2},U_2,V_2\right)du_1du_2}{\sqrt{(1+\delta)^2+(u_1-u_2)^2}}+\right. \\ +\int\limits_{-\infty}^{\infty}\int\limits_{-\infty}^{\infty}\frac{m_y\left(u_1,\frac{1}{2},U_1,V_1\right)m'_y\left(u_2,\frac{1}{2},U_2,V_2\right)du_1du_2}{\sqrt{(1+\delta)^2+(u_1-u_2)^2}}+ \\ +\int\limits_{-\infty}^{\infty}\int\limits_{-\infty}^{\infty}\frac{m_y\left(u_1,-\frac{1}{2},U_1,V_1\right)m'_y\left(u_2,\frac{1}{2},U_2,V_2\right)du_1du_2}{\sqrt{(2+\delta)^2+(u_1-u_2)^2}}+ \\ \left.+\int\limits_{-\infty}^{\infty}\int\limits_{-\infty}^{\infty}\frac{m_y\left(u_1,\frac{1}{2},U_1,V_1\right)m'_y\left(u_2,-\frac{1}{2},U_2,V_2\right)du_1du_2}{\sqrt{\delta^2+(u_1-u_2)^2}}\right]. \quad (8)$$

Here, $\delta = d/L$. The stripe magnetization components m_y and m'_y are rewritten in dimensionless variables on the basis of Eq. (4). According to Eqs. (5)-(8), the total energy can be presented as

$$W_M(U_1,V_1,U_2,V_2) = \frac{\mu_0 b^2 M_S^2}{4\pi L} I(U_1,V_1,U_2,V_2). \quad (9)$$

The factor $I(U_1,V_1,U_2,V_2)$ is the sum of dimensionless integrals from the brackets in Eqs. (7)-(8).

It is important that in Eq. (5) , the term responsible for the interaction between the vortex core magnetizations is missing. In the vortex core, the magnetization does not lie in the plane and is perpendicular to the stripe surface at the center. We do not take into account this energy, assuming it to be low. Indeed, the core magnetic charge on the stripe surface is proportional to the core area. However, the characteristic linear size of the core is about ten nanometers; therefore, the core area is much smaller than the area of the regions with the surface charge on the lateral surfaces. Hence, the energy of dipole interaction between the cores can be ignored. Nevertheless, note that the energy of interaction between the cores should depend not only on the coordinate, but also on the polarities p_1, p_2.

Figure 3 shows the $I(U_1,V_1,U_2,V_2)$ dependence for the interesting cases. Near the global minima, dimensionless energy integral (9) is satisfactorily described by the approximate function:

$$I(U_1,V_1,U_2,V_2) \approx I_0 + \\ \approx \frac{k_x \Delta U^2}{2(1+0.06|\Delta U^3|)} + \frac{k_y \Delta V^2}{2(1+10\Delta V^4)} + \\ + \frac{k_{0y} V_1^2}{2(1+60\Delta V_1^4)} + \frac{k_{0y} V_2^2}{2(1+60\Delta V_2^4)}. \quad (10)$$

Here, $\Delta U = U_1 - U_2 + u_0$, $\Delta V = V_1 - V_2 + v_0$, u_0, and v_0 are the coordinate differences of the equilibrium core position, I_0 is a constant determined by the level of the energy, k_{0y} is a constant that determines the magnitude of the restoring force at the displacement of the core along the axis y, kx, ky are constants, determining the interaction force between the cores in the projection on the x axis and the y axis, respectively. The numerical calculation of the integral $I(U_1,V_1,U_2,V_2)$ showed that near the minima, the parameters q and s only determine the free term I_0 and equilibrium core position. The rest parameters in Eq. (10) are determined also, according to Eq. (4), by the δ_c and δ_w values. The potential well curvature remains almost invariable at any q and s combinations. It means that, at the slight displacements of the core from the equilibrium position, the arising restoring force is independent of q and s. Figure 4 shows the comparison of empirical formula (10) with the numerical calculation. It can be seen that Eq. (10) is qualitatively consistent with the data numerically calculated using Eq. (9) and agrees satisfactorily with the results reported in [6,12,13,46] for a single stripe. Near the minima, good quantitative agreement is observed. In further calculations, assuming the core displacements to be slight, we use Eq. (10)in the quadratic approximation on the coordinates.

3 Cyclic Motion of a Vortex Wall Now, let us consider the behavior of the vortex core in an ac magnetic field applied in the stripe plane.

As was mentioned above, in the field of central forces, the magnetic vortex core behaves as a Larmor particle. The dynamic behavior of magnetic vortices is described well by the Thiele equation [31]. The system of Thiele equations for the VWs of two stripes has the form

$$\begin{cases} \mathbf{G}_1 \times \mathbf{v}_1 - D\mathbf{v}_1 - \nabla W_1 = 0, \\ \mathbf{G}_2 \times \mathbf{v}_2 - D\mathbf{v}_2 - \nabla W_2 = 0. \end{cases} \quad (11)$$

Here, $\mathbf{G}_\alpha = \pi_{T_\alpha} G_0(1 - p_\alpha h)\mathbf{k}$ is the gyrovector ($\mathbf{k}$ is the unit vector along the z axis, and $G_0 = 2\pi M_S b/\gamma$), $\mathbf{v}$ is the core velocity, and D is the effective viscous friction coefficient. The subscripts indicate the stripe (first or second) a vortex belongs to. The third term in the left-hand side of Eq. (11) is responsible for the nondissipative forces acting on the vortex core as a quasiparticle. Among such forces are the restoring force, force of interaction with the vortex core in the neighboring stripe, and effective force caused by the interaction between the vortex magnetization and external magnetic field. Thus, we have $W_\alpha = W_M(\mathbf{r}_1,\mathbf{r}_2) + W_{\alpha_H}$. Here, W_{α_H} is the Zeeman energy of a VW in the stripe with number α.

Then, taking into account (9) and (10), for the generalized forces acting on the vortex cores, we can write ($\mathbf{i}$ and $\mathbf{j}$ are the unit vectors along the x and y axes, respectively)

$$\mathbf{F}_\alpha(\mathbf{r}_1,\mathbf{r}_2) = -\nabla W_\alpha = -\kappa_x(U_1 - U_2)\mathbf{i} - \\ -\kappa_y(V_1 - V_2)\mathbf{j} - \chi V_\alpha \mathbf{j} + \mathbf{F}_{\alpha_H}. \quad (12)$$

Here, we used the designations $\kappa_x = \mu_0 M_S^2 b^2 k_x/(4\pi L)$, $\kappa_y = \mu_0 M_S^2 b^2 k_y/(4\pi L)$, $\chi = \mu_0 M_S^2 b^2 k_{0y}/(4\pi L)$. The effective force $\mathbf{F}_{\alpha_H}$ acting on the core in an ac magnetic field is perpendicular to the direction of this field and lies in the stripe plane. A specific direction of this force is determined by the vortex chirality q_α [47,48].

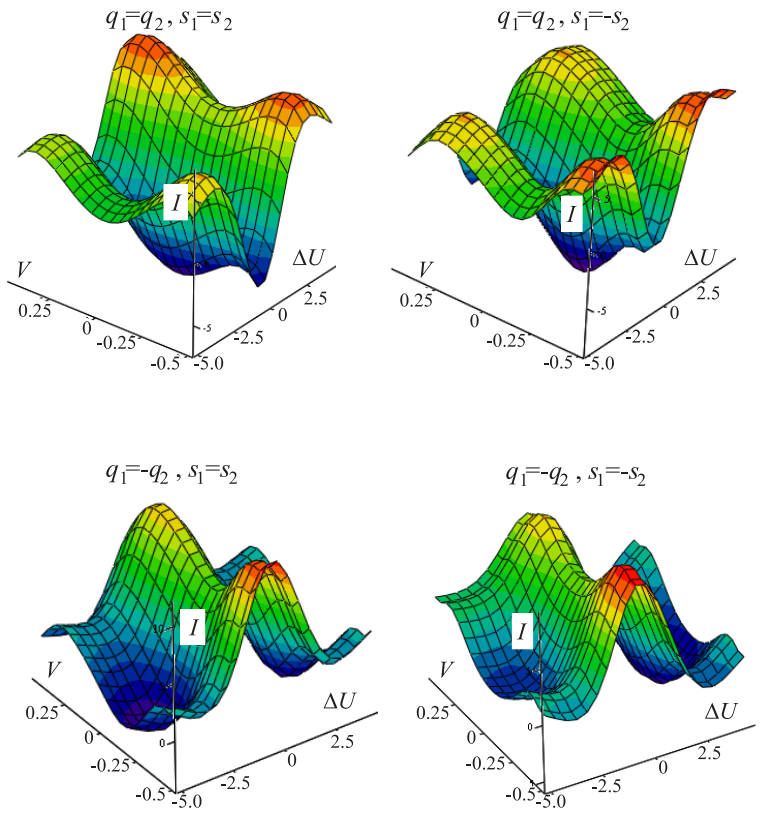

Figure 3 Profile of the dimensionless energy factor of a pair of interacting vortex walls. The surfaces are built for the case $V = V_1 = -V_2$. Here and below, the color shows the values of I.

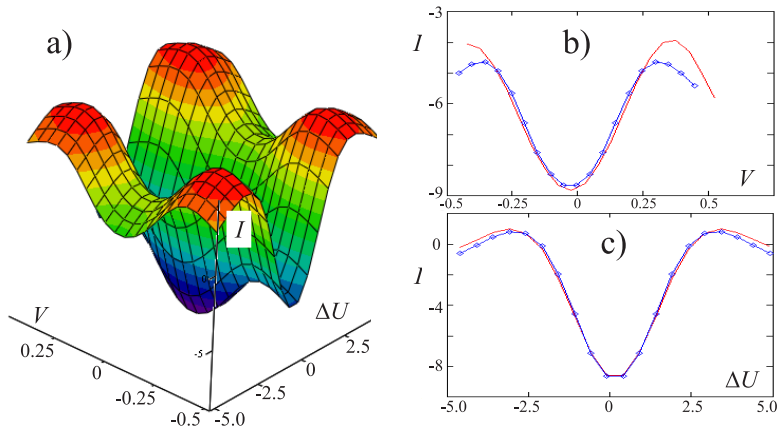

Figure 4 (a) Profile of the dimensionless energy factor for a pair of interacting vortex walls plotted using formula (10).Comparison of the numerical calculation of the dimensionless integral at $q_1 = q_2$ and $s_1 = s_2$ with empirical formula (10) in the cross sections (b) $\Delta U = 0$ and (c) $V = 0$. Here $V = V_1 = -V_2$.

Being projected onto the system of coordinates (local for each stripe), system (11) takes the form

$$\begin{cases} -G_1 v_{y_1} - D v_{x_1} - \kappa_x (x_1 - x_2) = -F_{1_x}, \\ G_1 v_{x_1} - D v_{y_1} - \kappa_y (y_1 - y_2) - \chi y_1 = -F_{1_y}, \\ -G_2 v_{y_2} - D v_{x_2} - \kappa_x (x_2 - x_1) = -F_{2_x}, \\ G_2 v_{x_2} - D v_{y_2} - \kappa_y (y_2 - y_1) - \chi y_2 = -F_{2_y}. \end{cases} \tag{13}$$

Here, F_{α_x} and F_{α_y} are the projections of force $\mathbf{F}_{\alpha_H}$ acting on the vortex cores due to the presence of the ac field component. Let the ac field be changing in accordance with the law $\mathbf{F}_{\alpha_H} = q_\alpha \mathbf{F}_0 \left(e^{i\omega t} + e^{-i\omega t}\right)$, ω be the cyclic field variation frequency, and $\mathbf{F}_0$ be the field amplitude.

We choose the trial solutions of system (13) in the form $x_\alpha = x_{0_\alpha}\left(e^{i\pi_{T_\alpha}\omega t + \phi_{\alpha_x}} + e^{-i\pi_{T_\alpha}\omega t - \phi_{\alpha_x}}\right)$, $y_\alpha = i y_{0_\alpha}\left(e^{i\pi_{T_\alpha}\omega t + \phi_{\alpha_y}} - e^{-i\pi_{T_\alpha}\omega t - \phi_{\alpha_y}}\right)$. Here, i is the unit imaginary number and $\phi_{\alpha_{x,y}}$ is the phase difference between the law of variation in the force $\mathbf{F}_{\alpha_H}$ and laws of the variation in coordinates x and y, respectively. Then, substituting the trial solutions into Eq. (13), we obtain for the steady-state regime

$$\begin{cases} G_0(1-p_1h)\omega y_{0_1} - (\kappa_x + iD\omega)x_{0_1} - \kappa_x x_{0_2} = F_{0_x} q_1, \\ G_0(1-p_1h)\omega x_{0_1} - (\kappa_y + \chi + iD\omega)y_{0_1} - \\ -\pi_{T_1}\pi_{T_2}\kappa_y y_{0_2} = -i\pi_{T_1} F_{0_y} q_1, \\ G_0(1-p_2h)\omega y_{0_2} - (\kappa_x + iD\omega)x_{0_2} - \kappa_x x_{0_1} = F_{0_x} q_2, \\ G_0(1-p_2h)\omega x_{0_2} - (\kappa_y + \chi + iD\omega)y_{0_2} - \\ -\pi_{T_1}\pi_{T_2}\kappa_y y_{0_1} = -i\pi_{T_2} F_{0_y} q_2. \end{cases} \tag{14}$$

Solving this system, we determine the complex amplitudes

$$\begin{aligned} x_{0_1} &= -\frac{C_x}{G_0(1-p_1h)^3(1-p_2h)^3 Z}, \\ y_{0_1} &= -\frac{C_y}{G_0(1-p_1h)^3(1-p_2h)^3 Z}. \end{aligned} \tag{15}$$

Here, we introduced the designations

$$\begin{aligned} C_x = {} & [F_{0_x}\left(q_1(\omega_y + \Omega + i\omega\omega_\Gamma)(1-p_2h) - \right. \\ & \left. -p_2\pi_{T_1}\omega_y(1-p_1h)\right) - iF_{0_y}p_1\omega(1-p_1h)(1-p_2h)\big] \times \\ & \times [(\omega_x + i\omega\omega_\Gamma)(\omega_y + \Omega + i\omega\omega_\Gamma)(1-p_1h) + \\ & + \pi_{T_1}\pi_{T_2}\omega_x\omega_y(1-p_2h) - \omega^2(1-p_1h)(1-p_2h)^2\big] + \\ & + [F_{0_x}\left(q_2(\omega_y + \Omega + i\omega\omega_\Gamma)(1-p_1h) - \right. \\ & \left. -p_1\pi_{T_2}\omega_y(1-p_2h)\right) - iF_{0_y}p_2\omega(1-p_1h)(1-p_2h)\big] \times \\ & \times [\omega_x(\omega_y + \Omega + i\omega\omega_\Gamma)(1-p_2h) + \\ & + \pi_{T_1}\pi_{T_2}(\omega_x + i\omega\omega_\Gamma)\omega_y(1-p_1h)\big], \end{aligned} \tag{16}$$

$$\begin{aligned} C_y = {} & [F_{0_x}\left(q_1(\omega_y + \Omega + i\omega\omega_\Gamma)(1-p_2h) - \right. \\ & \left. -p_2\pi_{T_1}\omega_y(1-p_1h)\right) - iF_{0_y}p_1\omega(1-p_1h)(1-p_2h)\big] \times \\ & \times [\omega_x(\omega_y + \Omega + i\omega\omega_\Gamma)(1-p_1h) + \\ & + \pi_{T_1}\pi_{T_2}\omega_y(\omega_x + i\omega\omega_\Gamma)(1-p_2h)] + \\ & + [F_{0_x}\left(q_2(\omega_y + \Omega + i\omega\omega_\Gamma)(1-p_1h) - p_1\pi_{T_2}\omega_y(1-p_2h)\right) - \\ & - iF_{0_y}p_2\omega(1-p_1h)(1-p_2h)\big] \times \\ & \times [(\omega_x + i\omega\omega_\Gamma)(\omega_y + \Omega + i\omega\omega_\Gamma)(1-p_2h) + \\ & + \pi_{T_1}\pi_{T_2}\omega_x\omega_y(1-p_1h) - \omega^2(1-p_1h)^2(1-p_2h)\big], \end{aligned} \tag{17}$$

$$\begin{aligned} Z = {} & \omega^4 - \omega^2\left[(\omega_x + i\omega\omega_\Gamma)(\omega_y + \Omega + i\omega\omega_\Gamma) \times \right. \\ & \left. \times \left(\frac{1}{(1-p_1h)^2} + \frac{1}{(1-p_2h)^2}\right) + \frac{2\pi_{T_1}\pi_{T_2}\omega_x\omega_y}{(1-p_1h)(1-p_2h)}\right] + \\ & + \frac{[(\omega_x + i\omega\omega_\Gamma)^2 - \omega_x^2][(\omega_y + \Omega + i\omega\omega_\Gamma)^2 - \omega_y^2]}{(1-p_1h)^2(1-p_2h)^2}, \end{aligned} \tag{18}$$

where $\omega_\Gamma = D/G_0$ is the dimensionless quantity, $\Omega = \chi/G_0$, $\omega_x = \kappa_x/G_0$, and $\omega_y = \kappa_y/G_0$.

The phase difference between the laws of variation in the exciting force and laws of the vortex core motion is determined from the expressions

$$\begin{cases} \sin(\phi_{\alpha_x}) = \dfrac{\mathrm{Im}(x_{0_\alpha})}{|x_{0_\alpha}|}, \\ \cos(\phi_{\alpha_x}) = \dfrac{\mathrm{Re}(x_{0_\alpha})}{|x_{0_\alpha}|}. \end{cases} \quad \begin{cases} \sin(\phi_{\alpha_y}) = \pi_{T_\alpha}\dfrac{\mathrm{Im}(y_{0_\alpha})}{|y_{0_\alpha}|}, \\ \cos(\phi_{\alpha_y}) = \pi_{T_\alpha}\dfrac{\mathrm{Re}(y_{0_\alpha})}{|y_{0_\alpha}|}. \end{cases} \tag{19}$$

It is interesting to discuss a simple particular case of a negligible damping $\omega_\Gamma = 0$. In this case, the mode eigenfrequencies can be determined from the condition $Z = 0$. As a result, we obtain

$$\begin{aligned} \omega_s^2 = {} & \omega_x\Omega\left(\tfrac{1}{(1-p_1h)^2} + \tfrac{1}{(1-p_2h)^2}\right) + \\ & + \omega_x\omega_y\left(\tfrac{\pi_{T_1}}{1-p_1h} + \tfrac{\pi_{T_2}}{1-p_2h}\right)^2. \end{aligned} \tag{20}$$

The polarity and chirality distributions and frequency values are given in Table 1. Since both stripes in the pair have the same sizes and magnetic characteristics, the G_0, D, and χ values for the stripes are analogous. This leads to the frequency degeneracy of the states. In particular, are twofold degenerate and states 3 and 4 are fourfold degenerate. As a result, we have six eigenfrequencies.

In the absence of a perpendicular dc field ($h = 0$), using expression (20) we obtain for the resonance frequencies

$$\omega_s = \sqrt{2\omega_x\Omega + 2\omega_x\omega_y\left(1 + \pi_{T_1}\pi_{T_2}\right)}. \tag{21}$$

The states with certain combinations of the chiralities, but opposite polarities in zero field h do not differ. Hence, at $\omega_\Gamma \to 0$ the degree of degeneracy is enhanced. As a result,

Table 1 Set of eigenfrequencies ω_s of the system calculated using Eq. (20) at different combinations of polarities and chiralities of the vortex walls.

No	$\{p_1, p_2, q_1, q_2\}$	ω_s
1	$\{1, 1, \pm1, \pm1\}$	$2\omega_x(\Omega + 2\omega_y)/(1-h)^2$
2	$\{1, 1, \pm1, \mp1\}$	$2\omega_x\Omega/(1-h)^2$
3	$\{\pm1, \mp1, 1, 1\}$, $\{\pm1, \mp1, -1, -1\}$	$2\omega_x\left(\Omega(1+h^2) + 2\omega_y h^2\right)/(1-h^2)^2$
4	$\{\pm1, \mp1, 1, -1\}$, $\{\pm1, \mp1, -1, 1\}$	$2\omega_x\left(\Omega(1+h^2) + 2\omega_y\right)/(1-h^2)^2$
5	$\{-1, -1, \pm1, \pm1\}$	$2\omega_x\left(\Omega + 2\omega_y\right)/(1+h)^2$
6	$\{-1, -1, \pm1, \mp1\}$	$2\omega_x\Omega/(1+h)^2$

the sets of states 1, 4, 5 and, separately, 2, 3, 6 from Table 1 become indistinguishable. Note that, in the absence of dc field h the difference between the polarities and chiralities is not as important as the difference between their products π_{T_α}, which is reflected in formula (21) suggesting that, at $h = 0$ there are only two different frequencies, $\omega_s = \sqrt{2\omega_x\Omega}$ and $\omega_s = \sqrt{2\omega_x\Omega + 4\omega_x\omega_y}$. In study [49] the dynamics of two interacting vortices in one stripe was theoretically analyzed. The authors obtained the result for a collective vortex motion frequency, which is a particular case of formula (21).

The power absorbed by a pair of stripes can be estimated as

$$P(\omega, h) \approx D\omega^2 \left(|x_{0_1}|^2 + |y_{0_1}|^2 + |x_{0_2}|^2 + |y_{0_2}|^2\right). \tag{22}$$

The dependences of the absorbed power on the frequency of an external ac field applied along the y and x axes are shown in Figs. 5 and 6, respectively. These plots need in our comments.

First of all, note that the investigated stripes are long and the VWs are distant from the ends. Therefore, the magnetic energy of an isolated stripe does not change at the vortex core displacement along the x axis. Therefore, the restoring force is not induced along the x axis. Upon displacement of the vortex core of a single stripe along the y axis, the magnetic subsystem energy changes because of the redistribution of magnetic charges on the stripe lateral surfaces. Thus, the restoring force arises along the y axis, regardless of the closeness to the second stripe. This feature is reflected in the character of wall motion in an ac magnetic filed.

The state illustrated in Fig. 5a does not exhibit the resonance properties. Depending on the mutual orientation of a perpendicular dc field h and core polarity p_α, we have the frequency dependences monotonically descending at different rates. The calculation of the difference between phases of the wall core motion in stripes 1 and 2 using formulas (19) showed that the rotation occurs synchronously ($\phi_{1_x} = \phi_{2_x}$ and $\phi_{1_y} = \phi_{2_y}$). At such combinations of the vortex polarities and chiralities, the DWs do not interact, since, at any instant of time, the conditions $\Delta U = 0$ and $\Delta V = 0$ are met. In this case, the equations of motion do not contain the restoring force projection along the x axisand the system is not oscillatory.

The similar effect can be observed in the case of an ac field applied along the y axis (Figs. 6a and 6b). The calculation of phases for these combinations $\{p_1, p_2, q_1, q_2\}$ showed that the coordinates U_1 and U_2 change in time synchronously. This is indicative of the absence of restoring force along the x axis.

The system behaves differently when the coordinates U_1 and U_2 of the vortex centers change in time nonsynchronously. In this case, the generalized force of interaction between the cores has a nonzero projection onto the x axis. In other words, there is a restoring factor both along the y axis and along the x axis. Then, the system has all the features of an oscillatory one and the resonance states in an ac field are observed. Such combinations are illustrated in Figs. 5b, 5c, 5d, 6c, and 6d. The insets in the plots show the directions and phases of the vortex core motion at certain instants of time.

It is interesting to examine the states with the same chirality, but opposite polarities (Figs. 5c and 6c). When an ac field is applied along the y axis, the resonance peak is only observed in a dc field perpendicular to the stripe plane. If an ac field is applied along the x axis, the resonance is implemented in any perpendicular fields h. In these states, the phase shift between the positions of stripe vortex centers $\phi_{1_{x,y}} - \phi_{2_{x,y}}$ depends on the frequency ω of an ac field and value of dc field h. This dependence is not observed at the rest $\{p_1, p_2, q_1, q_2\}$ combinations, where there are only two possible cases: $\phi_{1_{x,y}} - \phi_{2_{x,y}} = 0$ and π. The behavior of rotational phases of the stripe cores in the investigated case is shown in Fig. 7.

4 Conclusions In this article we discussed the specific features of the behavior of vortex domain wall in an ac magnetic field applied parallel to a pair of magnetostatically interacting stripes and across them. Our analysis and solution of equations of vortex motion showed that there exist certain combinations of the polarities and chiralities of the vortex walls at which there is resonance. Ignoring the damping, we obtained a simple expression for the resonant frequencies as functions of the vortex polarity, chirality and the value and direction of a dc magnetic field applied perpendicular to the stripe surface.

The knowledge of the states of interacting vortex walls, which exhibit the resonance or nonresonance behavior in ac fields, opens the opportunities for controlling the mag-

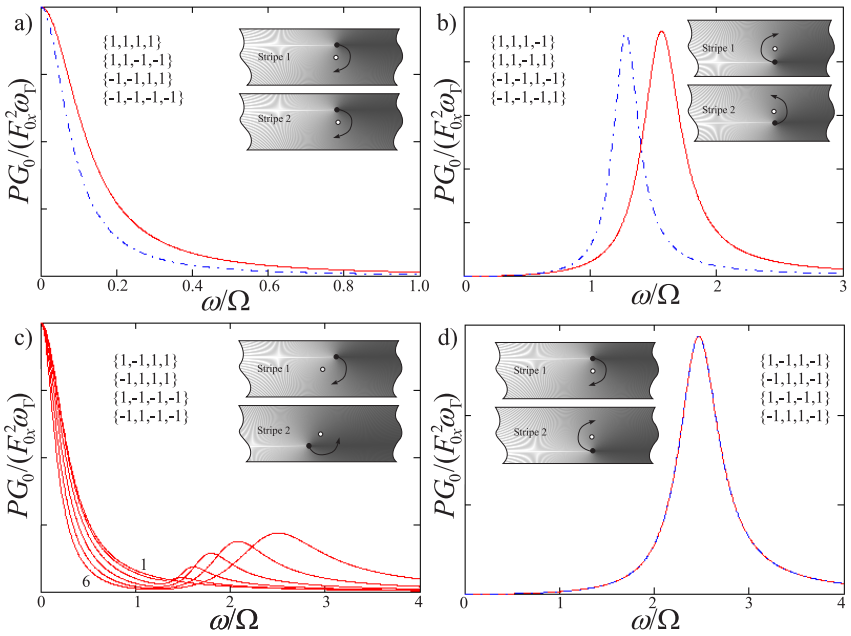

Figure 5 Dependence of the absorbed power (arb. units) on the ac field frequency. The ac field is applied along the y axis. The curves are plotted for the parameters $\omega_y = \Omega$, $\omega_x = \omega_y$, $\omega_\Gamma = 0.1$, and $h = 0.1$. (a, b) Power for the case of a dc field applied antiparallel to the z axis (dashed lines). (c, d) Dc field applied parallel and antiparallel to the z axis. (c) Set of curves 1-6 at dc fields of $h = 0...0.5$ with a step of $\Delta h = 0.1$. Inset: polarity and chirality combinations $\{p_1, p_2, q_1, q_2\}$ for the vortex walls and phases and directions of the vortex cores. Closed circles show the cores and open circles, the origins of coordinates.

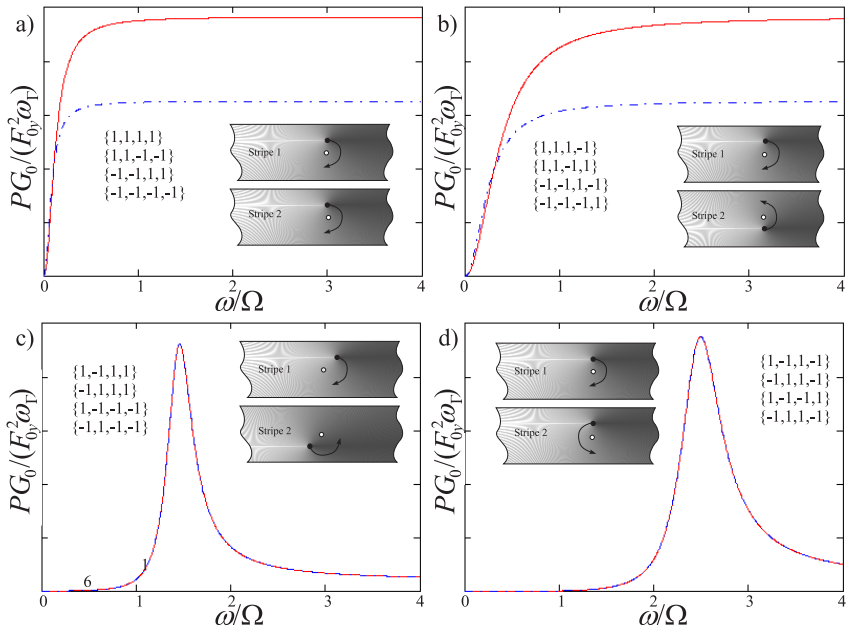

Figure 6 Dependence of the absorbed power (arb. units) on the frequency of ac field applied along the x axis. The curves are built for the same parameters as in Fig. 5.

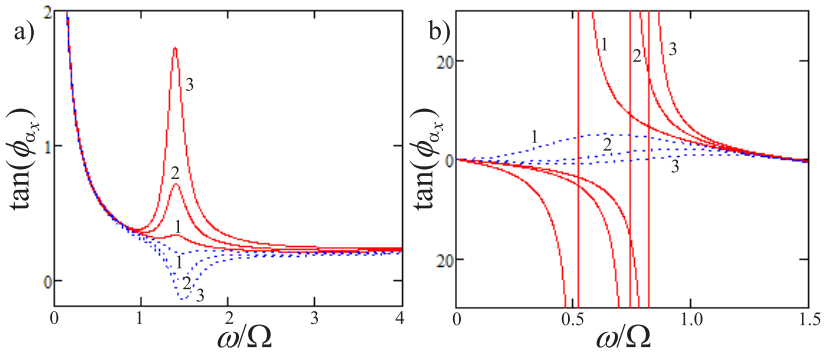

Figure 7 Dependence of the tangent of x-coordinate phase of the magnetic vortex core in stripe 1 (solid curves) and stripe 2 (dotted lines). Curves 1, 2, and 3 are built for perpendicular fields of $h_1 = 0.01$, $h_2 = 0.05$, and $h_3 = 0.1$, respectively. (a) Plot for the ac field applied along the y axis, and (b) plot for the ac field applied along the x axis.

netization of parallel stripe arrays. This is of great importance for the development of data storage devices.

The field dependence of the frequencies of collective vortex wall motion modes makes these systems candidates for application in various field sensors and other spintronic devices. The existence of the states with the resonant frequencies sensitive to the perpendicular field direction (Fig. 5b) offers a promising field for designing sensors capable of detecting both field value and direction.

Acknowledgements The reported study was funded by RFBR according to the research project no. 18-02-00161.

References

[1] D. A. Allwood, G. Xiong, C. C. Faulkner, D. Atkinson, D. Petit, R. P. Cowburn, *Science*, **2005**, *309*, 1688.
[2] M. Hayashi, L. Thomas, R. Moriya, Ch. Rettner, S.S.P. Parkin, *Science*, **2008**, *320*, 209.
[3] S. S. P. Parkin, M. Hayashi, L. Thomas, *Science*, **2008** *320*, 190.
[4] S. Jamet, N. Rougemaille, J. C. Toussaint, O. Fruchart, e-print arXiv:1412.0679v1 [cond-mat.mes-hall] **2014**.
[5] A. Thiaville, Yo. Nakatani, *Appl. Phys.* **2006** *101*, 161.
[6] H. Youk, G.-W. Chern, K. Merit, B. Oppenheimer, O. Tchernyshyov, *J. Appl. Phys* **2006**, *99*, 08B101.
[7] Yo. Nakatani, A. Thiaville, J. Miltat, *JMMM* **2005**, *290-291*, 750.
[8] V. D. Nguyen, O. Fruchart, S. Pizzini, J. Vogel, J.-C. Toussaint, N. Rougemaille, *Sci. Rep.* **2015**, *5*, 12417.
[9] N. Rougemaille, V. Uhlir, O. Fruchart, S. Pizzini, J. Vogel, J. C. Toussaint, *Appl. Phys. Lett.* **2012**, *100*, 172404.
[10] A. Janutka, *Acta Phys. Pol. A* **2013**, *124*, 641.
[11] A. G. Kozlov, M. E. Stebliy, A. V. Ognev, A. S. Samardak, A. V. Davydenko, L. A. Chebotkevich, *JMMM* **2017**, *422*, 452.
[12] D. J. Clarke, O. A. Tretiakov, G.-W. Chern, Ya. B. Bazaliy, O. Tchernyshyov, *Phys. Rev. B* **2008**, *78*, 134412.
[13] Y. Su, J. Sun, J. Hu, H. Lei, *EPL* **2013**, *103*, 67004.
[14] S.-K. Kim, J.-Y. Lee, Y.-S. Choi, K. Yu. Guslienko, K.-S. Lee, *Appl. Phys. Lett.* **2008**, *93*, 052503.
[15] J. Yang, C. Nistor, G. S. D. Beach, J. L. Erskine, *Phys. Rev. B* **2008**, *77*, 014413.
[16] K. Yu. Guslienko, J.-Y. Lee, S.-K. Kim, *IEEE Tran. Magn.* **2008**, *44*, 3079.
[17] I. Purnama, M. Chandra Sekhar, S. Goolaup, W. S. Lew, *Appl. Phys. Lett.* **2011**, *99*, 152501.
[18] Ch. Murapaka, S. Goolaup, I. Purnama, W. S. Lewa, *Appl. Phys. Lett.* **2015**, *117*, 053913.
[19] K. Yu. Guslienko, *J. Nanosci. Nanotechnol.* **2008**, *8*, 2745
[20] O. Tchernyshyov, *Ann. of Phys.* **2015**, *366*, 98.
[21] O. Klein, G. de Loubens, V. V. Naletov, F. Boust, T. Guillet, H. Hurdequint, A. Leksikov, A. N. Slavin, V. S. Tiberkevich and N. Vukadinovic, *Phys. Rev. B* **2008**, *78*, 144410.
[22] K.-S. Lee and S.-K. Kim, *Appl. Phys. Lett.* **2007**, *91*, 132511.
[23] B.A. Ivanov and G.M. Wysin, *Phys. Rev. B* **2002**, *65*, 134434.
[24] K.Yu. Guslienko, B.A. Ivanov, V. Novosad, Y. Otani, H. Shima, K. Fukamichi, *J. of Appl. Phys.* **2002**, *91*, 8037.
[25] V. A. Orlov, R. Yu. Rudenko, A. V. Kobyakov, A. V. Lukyanenko, P. D. Kim, V. S. Prokopenko, I. N. Orlova, *JETP* **2018**, *126*, 523.
[26] A. K. Zvezdin, V. I. Belotelov, K. A. Zvezdin, *JETP Letters* **2008**, *87*, 381.
[27] N. Locatelli, A. E. Ekomasov, A. V. Khvalkovskiy, Sh. A. Azamatov, K. A. Zvezdin, J. Grollier, E. G. Ekomasov, V. Cros, *Appl. Phys. Lett.* **2013**, *102*, 062401.
[28] F. Abreu Araujo, M. Darques, K. A. Zvezdin, A. V. Khvalkovskiy, N. Locatelli, K. Bouzehouane, V. Cros, L. Piraux, *Phys. Rev. B* **2012**, *86*, 064424.
[29] A. D. Belanovsky, N. Locatelli, P. N. Skirdkov, F. Abreu Araujo, J. Grollier, K. A. Zvezdin, V. Cros, A. K. Zvezdin, *Phys. Rev. B* **2012**, *85*, 100409(R).
[30] A. K. Zvezdin, K. A. Zvezdin, *Bulletin of the Lebedev Physics Institute* **2010**, *37*, 240.
[31] A. Thiele, *Phys. Rev. Lett.* **1973**, *30*, 230.
[32] J. Kim and S.-B. Choe, *J. of Magn.* **2007**, *12(3)*, 113.
[33] R. D. McMichael, M. J. Donahue, *IEEE Trans. Magn.* **1997**, *33*, 4167.
[34] O. A. Tretiakov, D. Clarke, Gia-Wei Chern, Ya. B. Bazaliy, O. Tchernyshyov, *Phys. Rev. Lett.* **2008**, *100*, 127204.

[35] M. N. Dubovik, B. N. Filippov, L. G. Korzunin, *Phys. Met. Metallogr.* **2016**, *117*, 329.
[36] G.-W. Chern, H. Youk, O. Tchernyshyov, *J. Appl. Phys.* **2006**, *99*, 08Q505.
[37] J. He, Z. Li, S. Zhang, *Phys. Rev. B* **2006**, *73*, 184408.
[38] U. K. Rossler, A. N. Bogdanov, K.-H. Muller, *IEEE Tran. Magn.* **2002**, *38*, 2586.
[39] K. Yu. Guslienko, V. Novosad, Y. Otani, H. Shima, K. Fukamichi, *Phys. Rev. B* **2001**, *65*, 024414.
[40] V. P. Kravchuk, D. D. Sheka, *Phys. of Solid State* **2007**, *49*, 1923.
[41] P. D. Kim, V. A. Orlov, V. S. Prokopenko, S. S. Zamai, V. Ya. Prints, R. Yu. Rudenko, T. V. Rudenko, *Phys. of Solid State* **2015**, *57*, 30.
[42] S. Chikasumi, *Physics of Ferromagnetism* Syokabo, Tokyo, **1980**.
[43] K.Yu. Guslienko, X.F. Han, D.J. Keavney, R. Divan, S.D. Bader, *Phys. Rev. Lett.* **2006**, *96*, 067205.
[44] M. Wolf, U.K. Robler, R. Schafer, *JMMM* **2007**, *314*, 105.
[45] P. D. Kim, V. A. Orlov, R. Yu. Rudenko, V. S. Prokopenko, I. N. Orlova, S. S. Zamai, *JETP Letters* **2015**, *101*, 562.
[46] A. Janutka, *Acta Phys. Pol. A* **2013**, *124*, 23.
[47] S.-B. Choe, Y. Acremann, A. Scholl, A. Bauer, A. Doran, J. Stohr, H. A. Padmore, *Science* **2010**, *304*, 420.
[48] J.Y. Lee, K.S. Lee, S. Choi, K. Yu. Guslienko, S.-K. Kim, *Phys. Rev B* **2007**, *76*, 184408.
[49] Y. Talbi, Y. Roussigne, P. Djemia, M. Labrune, *Journal of Physics: Conference Series* **2010**, *200*, 042027.